

Accepted Manuscript

Effect of temperature on selenium removal from wastewater by UASB reactors

Paolo Dessì, Rohan Jain, Satyendra Singh, Marina Seder-Colomina, Eric D. van Hullebusch, Eldon R. Rene, Shaikh Ziauddin Ahammad, Alessandra Carucci, Piet N.L. Lens



PII: S0043-1354(16)30067-7

DOI: [10.1016/j.watres.2016.02.007](https://doi.org/10.1016/j.watres.2016.02.007)

Reference: WR 11820

To appear in: *Water Research*

Received Date: 5 November 2015

Revised Date: 19 January 2016

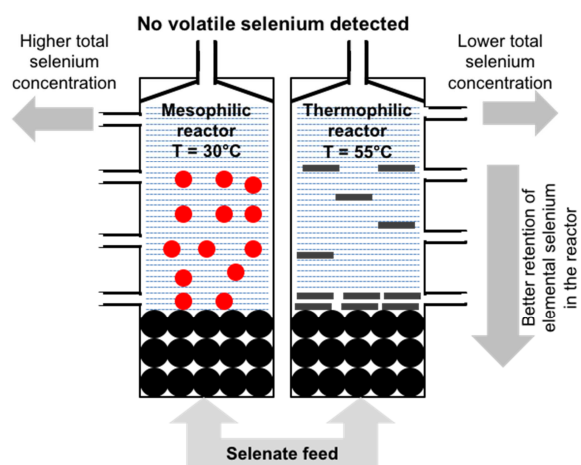
Accepted Date: 6 February 2016

Please cite this article as: Dessì, P., Jain, R., Singh, S., Seder-Colomina, M., van Hullebusch, E.D., Rene, E.R., Ahammad, S.Z., Carucci, A., Lens, P.N.L., Effect of temperature on selenium removal from wastewater by UASB reactors, *Water Research* (2016), doi: 10.1016/j.watres.2016.02.007.

This is a PDF file of an unedited manuscript that has been accepted for publication. As a service to our customers we are providing this early version of the manuscript. The manuscript will undergo copyediting, typesetting, and review of the resulting proof before it is published in its final form. Please note that during the production process errors may be discovered which could affect the content, and all legal disclaimers that apply to the journal pertain.

© <2016>. This manuscript version is made available under the CC-BY-NC-ND 4.0 license
<https://creativecommons.org/licenses/by-nc-nd/4.0/>

Graphical abstract



Effect of temperature on selenium removal from wastewater by UASB reactors

Paolo Dessì^{a,b,d}, Rohan Jain^{a,c,d*}, Satyendra Singh^e, Marina Seder-Colomina^{c,f}, Eric D. van Hullebusch^c, Eldon R. Rene^a, Shaikh Ziauddin Ahammad^e,
Alessandra Carucci^b, Piet N. L. Lens^{a,d}

^aUNESCO-IHE, Institute for Water Education, Westvest 7, 2611AX Delft, The Netherlands

^bDICAAR, Dept. of Civil-Environmental Engineering and Architecture, Piazza d'Armi,
09123 Cagliari, Italy

^cUniversité Paris-Est, Laboratoire Géomatériaux et Environnement (EA 4508), UPEM, 5,
Boulevard Descartes – Champs sur Marne, 77454 Marne-la-Vallée, France

^dDepartment of Chemistry and Bioengineering, Tampere University of Technology,
Korkeakoulunkatu 10, FI-33720 Tampere, Finland

^eDepartment of Biochemical Engineering and Biotechnology, Indian Institute of
Technology, Delhi, Hauz-Khas, 110016, New Delhi, India

^fInstitut de Minéralogie, de Physique des Matériaux, et de Cosmochimie (IMPMC).
Sorbonne Universités - UPMC Univ Paris 06, UMR CNRS 7590, Muséum National
d'Histoire Naturelle, IRD UMR 206, Paris, France.

*Corresponding author:

Phone: +31 152151715, fax: +31 152122921, e-mail: rohanjain.iitd@gmail.com, mail:

UNESCO-IHE, Institute for Water Education, Westvest 7, 2611AX Delft, The Netherlands

23 **Abstract**

24 The effect of temperature on selenium (Se) removal by upflow anaerobic sludge blanket
25 (UASB) reactors treating selenate and nitrate containing wastewater was investigated by
26 comparing the performance of a thermophilic (55°C) versus a mesophilic (30°C) UASB
27 reactor. When only selenate (50 µM) was fed to the UASB reactors (pH 7.3; hydraulic
28 retention time 8h) with excess electron donor (lactate at 1.38 mM corresponding to an
29 organic loading rate of 0.5 g COD L⁻¹ d⁻¹), the thermophilic reactor achieved a higher
30 total Se removal efficiency (94.4 ± 2.4%) than the mesophilic reactor (82.0 ± 3.8%). When
31 5000 µM nitrate was further added to the influent, total selenium removal was again better
32 under thermophilic (70.1 ± 6.6%) when compared to mesophilic (43.6 ± 8.8%) conditions.
33 The higher total effluent Se concentration in the mesophilic UASB reactor was due to the
34 higher concentrations of biogenic elemental Se nanoparticles (BioSeNPs). The shape of
35 the BioSeNPs observed in both UASB reactors was different: nanospheres and nanorods,
36 in respectively, the mesophilic and thermophilic UASB reactors. Microbial community
37 analysis showed the presence of selenate respirers as well as denitrifying
38 microorganisms.

39

40

41 **Keywords:** selenate, thermophilic, nitrate, selenium nanoparticles, UASB

42

43

44

45

46

47

48

49 **1. Introduction**

50 There is only one order of magnitude difference between the nutritional requirement (30 –
51 85 $\mu\text{g Se d}^{-1}$) and toxicity level (400 $\mu\text{g Se d}^{-1}$) of selenium (Se) for humans (Lenz and
52 Lens, 2009). Therefore, the United States Environmental Protection Agency (US EPA) has
53 set a discharge limit at 0.63 μM (50 $\mu\text{g Se L}^{-1}$) in drinking water (US EPA, Drinking water
54 contaminants). Both physical (nanofiltration, reverse osmosis) and chemical (ion
55 exchange, ferrihydrite adsorption and zero valent iron reduction) methods have been
56 tested for the removal of Se oxyanions from wastewaters (Lenz and Lens, 2009).
57 However, their application in full-scale systems is limited due to rather low efficiencies or
58 economic reasons. The microbial reduction of Se oxyanions to elemental Se in bioreactors
59 is a promising alternative to treat Se rich wastewater (Chung et al., 2006; Lenz et al.,
60 2008a). Biological reduction of Se oxyanions yields colloidal biogenic elemental Se
61 nanoparticles (BioSeNPs) that remove the Se oxyanions from the wastewater, although a
62 large fraction (25-68% of influent Se concentration) of these BioSeNPs remains present in
63 the effluent of the bioreactors (Lenz et al., 2008b). The presence of these BioSeNPs in the
64 effluent results in a higher total Se concentrations, and thus an additional post-treatment
65 step is required to meet the discharge limits (Buchs et al., 2013; Staicu et al., 2015)
66 thereby leading to higher operating costs.

67

68 One of the major reasons for the presence of BioSeNPs in the effluent is their extracellular
69 bio-production (Jain et al., 2015b). Dissimilatory reduction of selenium oxyanions by
70 selenate respiring microorganisms (e.g. *Sulfurospirillum barnesii*) leads to extracellular
71 production of BioSeNPs, while the detoxification of selenium oxyanions leads to their
72 intracellular production (Nancharaiah and Lens, 2015). The extracellular production of

73 BioSeNPs is known to be more pronounced when nitrate-grown microorganisms
74 (*Sulfurospirillum barnesii*, *Bacillus selenitireducens* and *Selenihalanaerobacter shriftii*) are
75 used to reduce selenite (Oremland et al., 2004). In many selenate containing wastewaters,
76 nitrate is present as well (e.g. agricultural drainage wastewater in the San Luis Drain that
77 disposes water in the Kesterson Reservoir in the San Joaquin Valley contains 48 mg L⁻¹
78 nitrate and 325 µg L⁻¹ selenium) (Tanji and Kielen, 2003) which might lead to a larger
79 extracellular production of BioSeNPs resulting in higher total Se concentrations in the
80 effluent when such wastewaters are treated by UASB reactors. However, so far no study
81 has been carried out to confirm this hypothesis in continuous bioreactors.

82

83 The microbial community present in a mesophilic UASB reactor, when fed with selenate,
84 evolved towards selenate respirers or dissimilatory reduction of selenate (Lenz et al.,
85 2009; Stolz et al., 2006). Under thermophilic conditions, a different microbial community
86 might evolve over time (Khemkhao et al., 2012), with different SeO₄²⁻ removal mechanism,
87 and thus different location. Furthermore, an elevated temperature can change the
88 allotrope (glass transition temperature of Se is 31°C), size (Lee et al., 2007; Tam et al.,
89 2010) and shape of Se nanoparticles (unpublished results), which may allow them to be
90 better retained in the UASB reactor. However, to the best of our knowledge, no study has
91 so far reported the microbial reduction of selenate under thermophilic conditions.

92

93 In this study, the biological reduction of selenate under thermophilic (55°C) conditions was
94 investigated in an upflow anaerobic sludge blanket (UASB) reactor inoculated with
95 anaerobic granular sludge. Another UASB reactor, operating at identical conditions but at
96 mesophilic (30°C) conditions, was used as a control. The effect of temperature on the
97 total, dissolved Se and selenate removal efficiency was determined, together with the

98 BioSeNPs concentration in the effluent and microbial communities present in the UASB
99 granules. The effect of nitrate at different influent concentrations (100, 500 and 5000 μM
100 corresponding to $\text{NO}_3^-/\text{SeO}_4^{2-}$ ratio = 2, 10 and 100, respectively) was also investigated.

101

102 **2. Materials and methods**

103 **2.1 Source of biomass**

104 The seed sludge used in this study, described in detail by Roest et al. (2005) was obtained
105 from a full scale UASB reactor treating wastewater of four paper mills (Industriewater
106 Eerbeek B.V., Eerbeek, The Netherlands). Both UASB reactors were inoculated with 200 g
107 wet weight anaerobic granular sludge, as described by Lenz et al. (2008a).

108

109 **2.2 Composition of the synthetic wastewater**

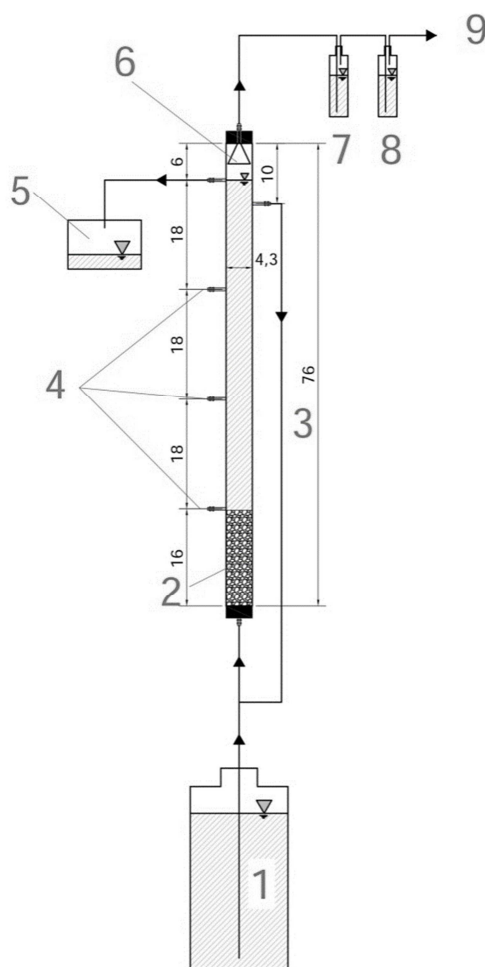
110 The composition of the synthetic wastewater was (in g L^{-1}): $\text{Na}_2\text{HPO}_4 \cdot 2\text{H}_2\text{O}$ (0.053),
111 KH_2PO_4 (0.041), NH_4Cl (0.300), $\text{CaCl}_2 \cdot 2\text{H}_2\text{O}$ (0.010), $\text{MgCl}_2 \cdot 6\text{H}_2\text{O}$ (0.010) and NaHCO_3
112 (0.040). 0.1 mL of the acid as well as alkaline trace metal solutions was added to 1 L of
113 the synthetic wastewater. The composition of acid and alkaline trace elements are
114 described in Stams et al. (1992).

115

116 **2.3 UASB setup**

117 Two UASB reactors (1 L volume) were operated at a hydraulic retention time (HRT) of 8 h
118 (Figure 1). The influent was fed from the bottom of the reactor and a recirculation ratio of 2
119 was maintained for mixing. The influent and recirculation flow were maintained constant at
120 2.2 and 4.4 mL min^{-1} , respectively, resulting in an upflow velocity of 0.3 m h^{-1} . The
121 thermophilic UASB reactor was maintained at 55 (± 2) $^\circ\text{C}$ using a water jacket, while the
122 mesophilic UASB reactor was maintained at 30 (± 2) $^\circ\text{C}$ in a temperature controlled room.

123 Two gas traps were connected to the exit of each UASB reactor. The first gas trap (G1)
124 contained 200 mL of concentrated HNO_3 to trap alkylated Se compounds and the second
125 gas trap (G2) contained 100 mL of 6 M NaOH to trap H_2Se (Lenz et al., 2008a). The
126 sampling ports of both reactors were named S1, S2 and S3, from the bottom to the top
127 (Figure 1).



128
129 **Figure 1.** Schematic overview and dimensions (in cm) of the UASB reactors used in this
130 study. Influent tank (1), anaerobic sludge (2), recirculation system (3), sampling ports S1,
131 S2 and S3 from the bottom to the top (4), effluent tank (5), gas separator (6), HNO_3 trap
132 (7), NaOH trap (8) and gas outlet (9).

133

134 **2.4 UASB operating conditions**

135 Five different operational periods were investigated in both reactors. Sodium lactate
 136 ($C_3H_5NaO_3$), Sodium selenate (Na_2SeO_4) and potassium nitrate (KNO_3) as a source of
 137 carbon, selenate and nitrate, respectively, were added at different concentrations during
 138 the experiment. The pH was maintained at 7.0-7.5 by the use of phosphate buffer in the
 139 influent. During period I (1-25 days), sodium selenate (Na_2SeO_4) was added to the influent
 140 solution at a concentration of 10 μM ($30 \mu M d^{-1}$), as operated in the study carried out by
 141 Lenz et al. (2008a).

142

143 **Table 1.** Different operating periods of the UASB reactors used in this study

Period	Operating days	Lactate influent conc. (mM)	SeO_4^{2-} influent conc. (μM)	NO_3^- influent conc. (μM)
I	1 - 25	1.38	10	0
II ^a	26 - 43	1.38	50	0
III	44 - 60	1.38	50	100
IV	61 - 82	1.38	50	500
V	83 - 98	13.8	50	5000

144 Note: ^a The reactors were inoculated with fresh biomass during this period

145

146 At the start of period II (26-43 days), both UASB reactors were re-inoculated with fresh
 147 anaerobic granules to avoid the interference of trapped Se in the biomass from period I
 148 when determining the BioSeNPs concentration along the reactor length. During period II,
 149 both UASB reactors were fed with a selenate concentration of 50 μM ($150 \mu M d^{-1}$).

150

151 During period III (44-60 days), nitrate (100 μM , $300 \mu M d^{-1}$) was added to the influent
 152 along with selenate (50 μM , $150 \mu M d^{-1}$) at a NO_3^- / SeO_4^{2-} ratio of 2. The influent

153 concentration of nitrate was increased 5 times ($500 \mu\text{M}$, $1500 \mu\text{M d}^{-1}$) during period IV
154 (61-82 days) which changed the $\text{NO}_3^- / \text{SeO}_4^{2-}$ ratio to 10. In the period V (83-98 days),
155 the influent nitrate concentration was increased to $5000 \mu\text{M}$ ($15000 \mu\text{M d}^{-1}$; $\text{NO}_3^- / \text{SeO}_4^{2-}$
156 ratio = 100).

157

158 Both UASB reactors were operated by supplying the electron donor lactate in excess
159 during the entire duration of the study to avoid the incomplete selenate and nitrate
160 reduction due to the lack of electron donor. The reactors were fed with a synthetic
161 wastewater containing 1.38 mM (corresponding to an organic loading rate of 0.5 g COD L^{-1}
162 d^{-1}) of sodium lactate as the sole electron donor till the end of period IV. The influent
163 lactate concentration was increased to 13.8 mM (corresponding to an organic loading rate
164 of $5 \text{ g COD L}^{-1} \text{ d}^{-1}$) during period V.

165

166 **2.5 Sampling**

167 50 mL of samples from the influent and effluent of both UASB reactors were collected
168 daily. To investigate the BioSeNPs stratification in the UASB reactors, samples were
169 collected every 2-3 days from different sampling ports during Period II (26-43 days).
170 Samples from the gas traps were analyzed for Se at the end of every period. Samples for
171 scanning electron microscopy–energy disperse X-ray analysis (SEM-EDXS) of the
172 BioSeNPs was collected from the effluent at the end of study (end of period V).

173

174 **2.6 DGGE analysis and sequencing**

175 A denatured gradient gel electrophoresis (DGGE) analysis followed by sequencing of
176 selected bands was carried out to describe the microbial populations in the reactors due to

177 their exposures to selenate, nitrate and two different operating temperatures. The DNA
178 extraction, polymerase chain reaction and denatured gradient gel electrophoresis has
179 been carried out as described in a previous study (Jain et al., 2016). The samples for
180 DGGE analysis were taken on day 0 (inoculum), day 43 (end of period II) and day 98 (end
181 of period V). Selected bands obtained in the DGGE analysis were excised from the gel.
182 The individually excised gel bands were further cut into smaller pieces with a sterile blade,
183 and kept overnight in 30 μ L of Tris-EDTA (TE) buffer at 4°C. The overnight incubated
184 samples at 4 °C were heated to 95 °C for 10 min to elute DNA into the buffer. Thereafter, 1
185 μ L of each of the eluted samples was used as a template in the next PCR, which was
186 carried out using the same primer but without the GC clamp. PCR amplification products
187 were checked on ethidium bromide stained 1.5% agarose gel before their sequencing. All
188 sequencing was carried out using the ABI Prism Big Dye Terminator Cycle Sequencing
189 Ready Reaction Kit on the ABI Prism 377 DNA sequencer (Applied Biosystems, Waltham,
190 Massachusetts). All sequence results were compared with known 16S rRNA sequences in
191 the GenBank database using the basic local alignment search tool (BLASTn).

192
193 The obtained band patterns were subjected to digital analysis by using XR+ Image Lab 2.0
194 software (Bio-Rad, Hercules, California). Peak areas of band patterns in the DGGE
195 fingerprints were used to indicate the intensities. The peaks that were detected were
196 adjusted to remove the unresolved peaks because of background, and the peaks with an
197 area < 1% of the maximum peak in a DGGE profile were excluded. The diversity analysis
198 was carried out using Gel Compar II version 6.6 (Applied Biomath, Sint-Martens-Latem,
199 Belgium). Dice coefficients, i.e. unweighted data on the basis of band presence or
200 absence, were calculated to have a better understanding of the banding patterns. A cluster

201 analysis using the unweighted pair group method with arithmetic mean (UPGMA) on the
202 basis of the Dice coefficient was performed.

203 **2.7 Analytics and statistics**

204 Samples of influent, effluent and from the sampling ports were analyzed for residual total
205 Se concentration, using an atomic absorption spectroscopy – Graphite Furnace (AAS-GF)
206 (ThermoElemental Solaar MQZe GF95) and a Se lamp at 196.0 nm. Samples taken from
207 the HNO₃ and NaOH gas traps were diluted two times with 6 M NaOH (G1) and 14.4 M
208 HNO₃ (G2), respectively, to adjust the pH before AAS-GF analysis. To separate the
209 BioSeNPs from liquid phase, 15 mL of the effluent was centrifuged for 10 min at 37,000g
210 (Hermle Z36 HK high speed centrifuge). The supernatant was analyzed by AAS-GF to
211 obtain the dissolved Se concentrations in the effluent. The BioSeNPs concentration in the
212 effluent was calculated by subtracting the dissolved Se concentration from the total Se
213 concentration in the effluent. The samples were acidified prior to measurement by adding
214 a few drops of concentrated HNO₃.

215

216 Selenate, nitrate and lactate in the influent and effluent were determined by Ion
217 Chromatography (IC) (Dionex ICS 1000), equipped with an AS4A column with an eluent
218 composition of 1.8 mM sodium carbonate and 1.7 mM sodium bicarbonate. The eluent
219 flow rate was maintained at 0.5 mL min⁻¹. The retention time of lactate, nitrate and
220 selenate was 1.3, 3.9 and 11.3 min, respectively. SEM-EDXS analysis was carried out
221 according to the protocol described in earlier study (Jain et al., 2015c).

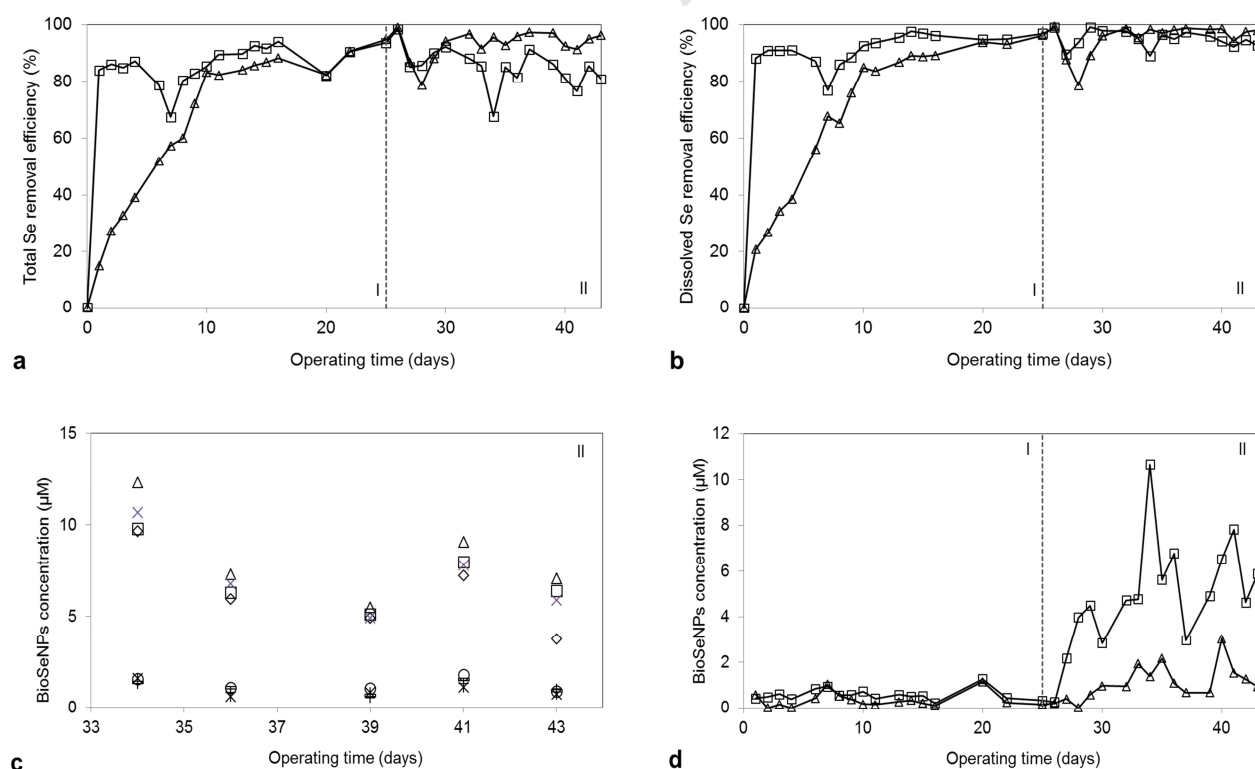
222

223 The average percentage removal and standard deviation were obtained by taking the last
224 five data points at the end of each period.

225

226 **3. Results**227 **3.1 Selenium removal in the absence of nitrate (Period I-II)**

228 The performance of both reactors was not similar during the first few days of operation (0-
229 9 days). The removal of selenium was almost instantaneous in the mesophilic reactor
230 (Figure 2a), achieving a total and dissolved Se removal efficiency of > 85% after the first
231 day of operation. The thermophilic reactor was able to achieve comparable efficiencies
232 only after a ~ 15 days adaptation period (Figure 2a). However, at the end of period I, the
233 removal efficiency of both the total and dissolved Se was nearly identical (~ 90% of 10
234 μM added selenate) for both UASB reactors, irrespective of their operational temperature
235 (Table S1 in SI). On day 25 of UASB reactor operation, the concentrations of total and
236 dissolved Se in the effluent of both UASB reactors were lower than the US EPA limit of
237 $0.63 \mu\text{M}$ Se for drinking waters (US EPA, Drinking water contaminants), but higher than
238 the flue gas desulfurization wastewater discharge criterion of $0.063 \mu\text{M}$ (US EPA, 2015).



239 **Figure 2.** Comparison between the total Se (a) and dissolved Se (b) removal efficiency
240 (%) in period I-II under mesophilic (30°C, □) and thermophilic (55°C, Δ) conditions. The
241 concentration of BioSeNPs (c) in the samples recovered from sampling ports S1 (◇), S2
242 (□), S3 (Δ) and effluent (×) of the mesophilic reactor and S1 (*), S2 (○), S3 (+) and effluent
243 (—) of thermophilic reactor and effluent BioSeNPs concentration (d) in the mesophilic
244 (30°C, □) and thermophilic (55°C, Δ) UASB reactor during period I-II. The vertical dotted
245 line represents the switch between the different operating periods.

246

247 In period II, higher selenate loading rates (5 times more than period I, 50 μM, 150 μM d⁻¹)
248 did not affect the Se removal efficiency of the mesophilic reactor and high total Se removal
249 efficiencies were obtained immediately (Figure 2a, Table S1 in SI). For the thermophilic
250 reactor, the removal of the total Se started instantaneously, in contrast to period I when
251 the influent selenate concentration was 5 times lower. In period II, the average removal
252 efficiency of the total Se after achieving steady state was 94.4 (± 2.4)% and 82.0 (± 3.8)%,
253 respectively, under thermophilic and mesophilic UASB conditions (Figure 2a, Table S1 in
254 SI). The average dissolved Se removal efficiency was better for the thermophilic (97.3 ±
255 1.7%) compared to mesophilic (93.9 ± 1.5%) UASB reactor (Figure 2b, Table S1 in SI).
256 The selenate removal efficiencies (> 99%) were similar for both the thermophilic and the
257 mesophilic UASB reactor (Figure S1a in SI, Table S1 in SI). Lactate was completely
258 consumed (> 99%) during this period of reactor operation (Figure S1b in SI).

259

260 **3.2 BioSeNPs concentration in the absence of nitrate (Period II)**

261 The BioSeNPs concentration measured in each sampling port (S1, S2 and S3) in the
262 thermophilic UASB reactor during period II was lower than the corresponding values
263 measured in the mesophilic UASB reactor (Figure 2c). The concentration of BioSeNPs

264 measured in the different ports of the thermophilic UASB reactor ranged between 0.6 and
 265 2 μM along the reactor height. On the other hand, the concentrations of BioSeNPs along
 266 the height of the mesophilic UASB reactor varied from 10 μM on day 34 to 5 μM on day 39
 267 (Figure 2c).

268

269 Figure 2d showed that the BioSeNPs concentration was consistently lower in the
 270 thermophilic UASB reactor effluent when compared to the mesophilic UASB reactor for
 271 period II and slightly lower in period I. The analysis of UASB reactor effluents suggests
 272 that the BioSeNPs fraction was 2.1% (56.2 μmol) and 9.2% (248.7 μmol), respectively, in
 273 the thermophilic and mesophilic reactor of the total Se fed (2700.0 μmol) during the entire
 274 period II (Table 2). During period I, the BioSeNPs fraction in the effluent of the thermophilic
 275 (4.0%) UASB reactor was also lower than in the mesophilic reactor (6.0%) (Table 2).

276

277 **Table 2.** Total BioSeNPs present in the effluent of thermophilic and mesophilic UASB
 278 reactors during different operational periods.

Period		I	II ^a	III	IV	V ^b
Operating days		1 - 25	26 - 43	44 - 60	61 - 82	83 - 98
Total Se fed (μmol)		750	2700	2550	3300	2400
Total BioSeNPs in	M ^c	44.8	248.7	172.3	316.4	710.1
effluent (μmol)	T ^d	29.8	56.2	142.0	164.7	402.4
% of BioSeNPs in the	M	6.0	9.2	6.7	9.6	29.6
effluent to total Se feed	T	4.0	2.1	5.6	5.0	16.8

279 Note: ^aThe reactors were inoculated with fresh anaerobic granules during this period;

280 ^bLactate concentration increased to 13.88 mM on day 85; ^cM refers to mesophilic and ^dT

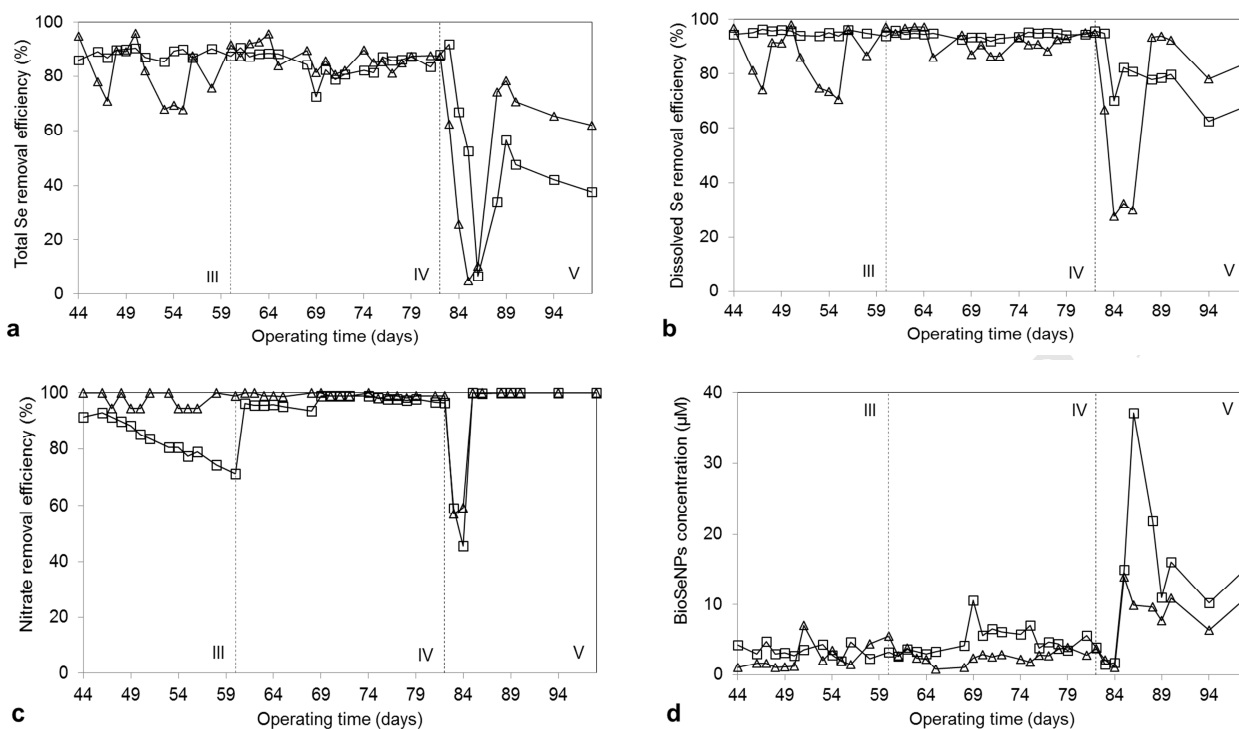
281 refers to thermophilic

282
283 **3.3 Selenium removal in the presence of nitrate (Period III-V)**

284 During period III (44 – 60 days), the addition of 100 μM ($300 \mu\text{M d}^{-1}$) of nitrate (NO_3^- /
285 SeO_4^{2-} ratio = 2) in the influent had very little effect or even slightly improved the Se
286 removal efficiency of the mesophilic reactor. Both the total ($88.8 \pm 1.5\%$) and dissolved
287 ($94.8 \pm 0.9\%$) Se removal efficiencies in the effluent of the mesophilic UASB reactor were
288 comparable to the concentrations measured prior to the addition of nitrate (Figures 3a, 3b
289 and Table S1 in SI). The selenate removal efficiency in the mesophilic reactor during
290 period III exceeded 99% (Figure S2a in SI). A decrease in the total ($73.6 \pm 8.5\%$) and
291 dissolved Se ($80.4 \pm 10.9\%$) removal efficiency was observed in the thermophilic UASB
292 reactor after the addition of 100 μM of nitrate (NO_3^- / SeO_4^{2-} ratio = 2) (Figure 3a and 3b,
293 Table S1 in SI). During the first 4 days of period III (days 44 - 47), the removal efficiency of
294 both the total and dissolved Se in the thermophilic UASB reactor effluent decreased by
295 ~10% after the addition of nitrate (Figures 3a and 3b). The selenate removal efficiency
296 ($85.1 \pm 10.9\%$) in the effluent of the thermophilic UASB reactor followed the same trend of
297 the dissolved Se (Table S1, Figure S2a in SI). The nitrate removal efficiency of the
298 thermophilic UASB reactor ($97 \pm 3.1\%$) was better than that of the mesophilic reactor (76.5
299 $\pm 3.7\%$), suggesting that the effluent nitrate concentration was below the detection limit of
300 ~ 16 μM (Figure 3c, Table S1 in SI). Lactate was completely consumed by both UASB
301 reactors at 1.38 mM (4.14 mM d^{-1}) of feed concentration (Figure S2b in SI).

302

303



304 **Figure 3.** Removal efficiency (%) of total Se (a), dissolved Se (b) and nitrate (c) during the
 305 nitrate fed periods III, IV and V (□ mesophilic, Δ thermophilic). Effluent BioSeNPs
 306 concentration (d) in the mesophilic (30°C, □) and thermophilic (55°C, Δ) UASB reactor
 307 during period III-V. The vertical dotted line represents the switch between the different
 308 operating periods.

309

310 During period IV (61 - 82 days), when the nitrate concentration was increased to 500 µM
 311 ($1500 \mu\text{M d}^{-1}$) and thus the $\text{NO}_3^- / \text{SeO}_4^{2-}$ ratio to 10, the removal efficiency of total Se
 312 ($86.1 \pm 1.8\%$), dissolved Se ($94.9 \pm 0.6\%$) and selenate ($> 99\%$) in the mesophilic UASB
 313 reactor was similar to the efficiency observed in period III (Figures 3a, 3b, Table S1 and
 314 Figure S2a in SI). The removal efficiencies of total Se ($85.3 \pm 2.6\%$), dissolved Se ($92.1 \pm$
 315 2.5%) and selenate ($95.6 \pm 6.1\%$) in the thermophilic UASB reactor in period IV improved
 316 when compared to period III and became comparable to the ones achieved in the
 317 mesophilic UASB reactor (Figures 3a, 3b, Table S1 and Figure S2a in SI). However, the

318 total Se and dissolved Se removal efficiency achieved in period IV for the thermophilic
319 reactor were still less than those achieved during period II in the same reactor. The
320 selenate removal efficiency was comparable in the thermophilic UASB reactor in periods II
321 and IV (Table S1, Figures S1a and S2a in SI). The nitrate removal efficiency in the
322 thermophilic and mesophilic UASB reactor were, respectively, 98.7 (\pm 0.3)% and 97.1 (\pm
323 0.6)%. This suggests that nitrate removal efficiencies were not affected in the thermophilic
324 UASB reactor, while improved in the mesophilic UASB reactor when compared to period
325 III (Figure 3c, Table S1 in SI). Lactate was completely consumed in both UASB reactors
326 during this period (Figure S2b in SI).

327

328 In period V (82 - 97 days), the influent nitrate concentration was increased by 10 times,
329 when compared to period IV, to achieve a $\text{NO}_3^- / \text{SeO}_4^{2-}$ ratio of 100. Both reactors had a
330 decreased efficiency at the outset when compared to period IV. The total Se removal
331 efficiency for the thermophilic UASB reactor ($70.1 \pm 6.6\%$), when compared to the
332 mesophilic UASB reactor ($43.6 \pm 8.8\%$), was better (Figure 3a, Table S1 in SI). The
333 dissolved Se removal efficiency for the thermophilic UASB reactor ($88.3 \pm 7.0\%$) was
334 marginally better than the one observed in the mesophilic UASB reactor ($73.7 \pm 7.6\%$)
335 (Figure 3b and Table S1 in SI). The selenate and nitrate removal efficiencies in both UASB
336 reactors exceeded 98 and 99%, respectively (Figures S2a and 3c). The lactate removal
337 efficiencies in period V was greater than 80% in both UASB reactors (Figure S2b). It is
338 important to note that lactate was not in excess on the first two days of period V.

339

340 **3.4 BioSeNPs concentration in the presence of nitrate (Period III-V)**

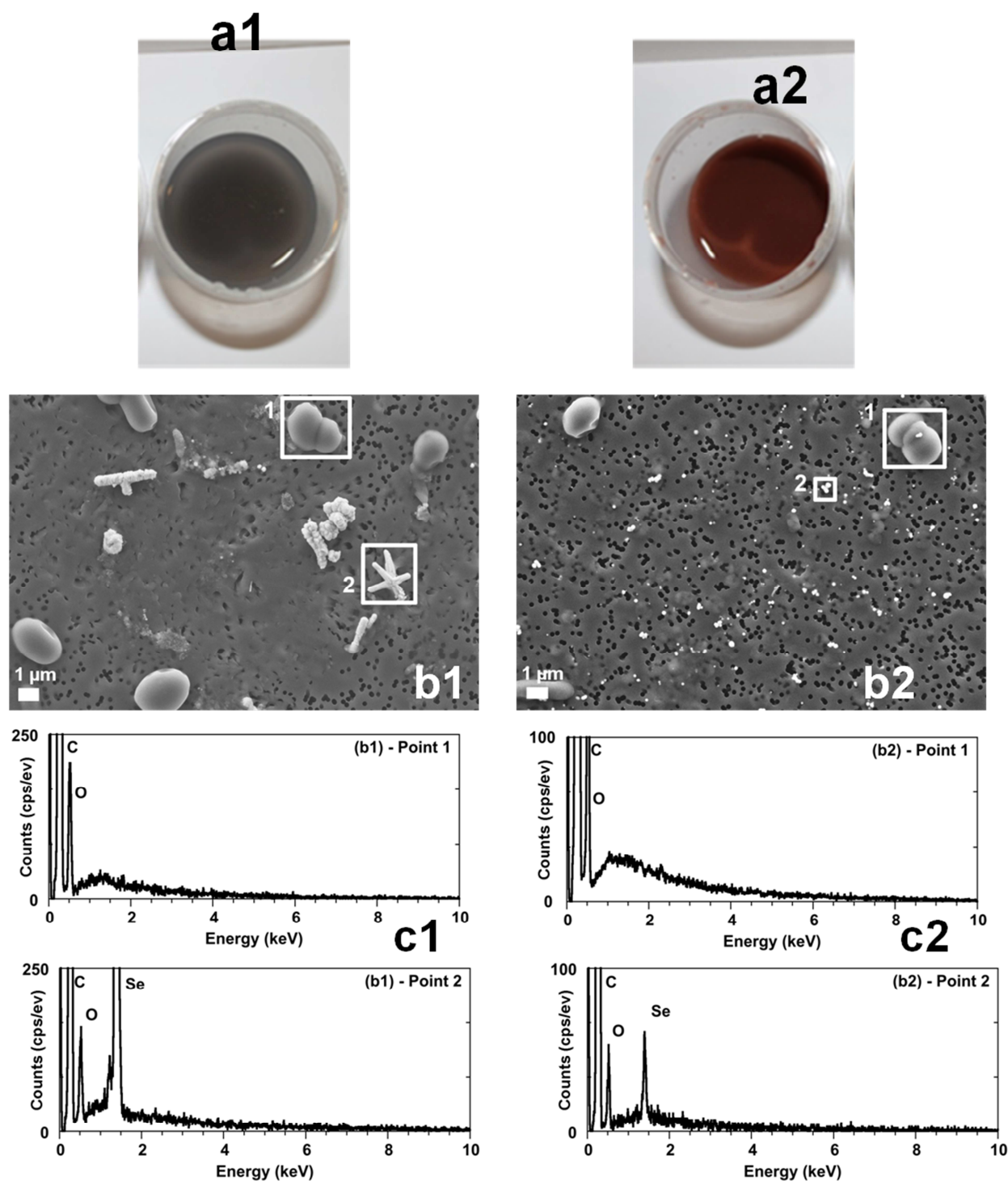
341 The concentration of BioSeNPs in the effluent of both UASB reactors during period III was
342 similar (Figure 3d, Table 2). However, during period IV and V, when the $\text{NO}_3^- / \text{SeO}_4^{2-}$

343 ratio was 10 and 100, respectively, the BioSeNPs concentration in the thermophilic UASB
344 reactor effluent was lower than in the mesophilic UASB reactor effluent (Table 2). It is
345 important to note that when compared to period II, BioSeNPs fraction in effluent increased
346 by more than 10% and 20% under, respectively, thermophilic and mesophilic operating
347 conditions after the addition of nitrate in the influent at 5000 μM ($\text{NO}_3^- / \text{SeO}_4^{2-}$ ratio =
348 100).

349

350 **3.5 Characteristics of the BioSeNPs in thermophilic and mesophilic UASB reactors**

351 The color of BioSeNPs present in the effluent of the thermophilic and mesophilic UASB
352 reactor was different from the day 1 onwards and remained different throughout the study
353 (Figure 4a). Grey colored BioSeNPs were observed in the thermophilic UASB reactor,
354 while they were red colored under mesophilic conditions. BioSeNPs present in the effluent
355 of the thermophilic UASB reactor were nanorods (Figure 4b1, Figure S3 in SI), whereas
356 those in the effluent of the mesophilic UASB reactor were spherical (Figure 4b2). The
357 effluents of both the UASB reactors showed that microorganisms were of similar shape
358 and were present in minor quantities (Figure 4b1 and 4b2). EDXS spectra confirmed that
359 the nanoparticles were composed of Se (Figures 4c1 and 4c2, Points 2), while the washed
360 out microorganisms in the effluent did not shown any Se peak (Figures 4c1 and 4c2,
361 Points 1).



362

363

364

365

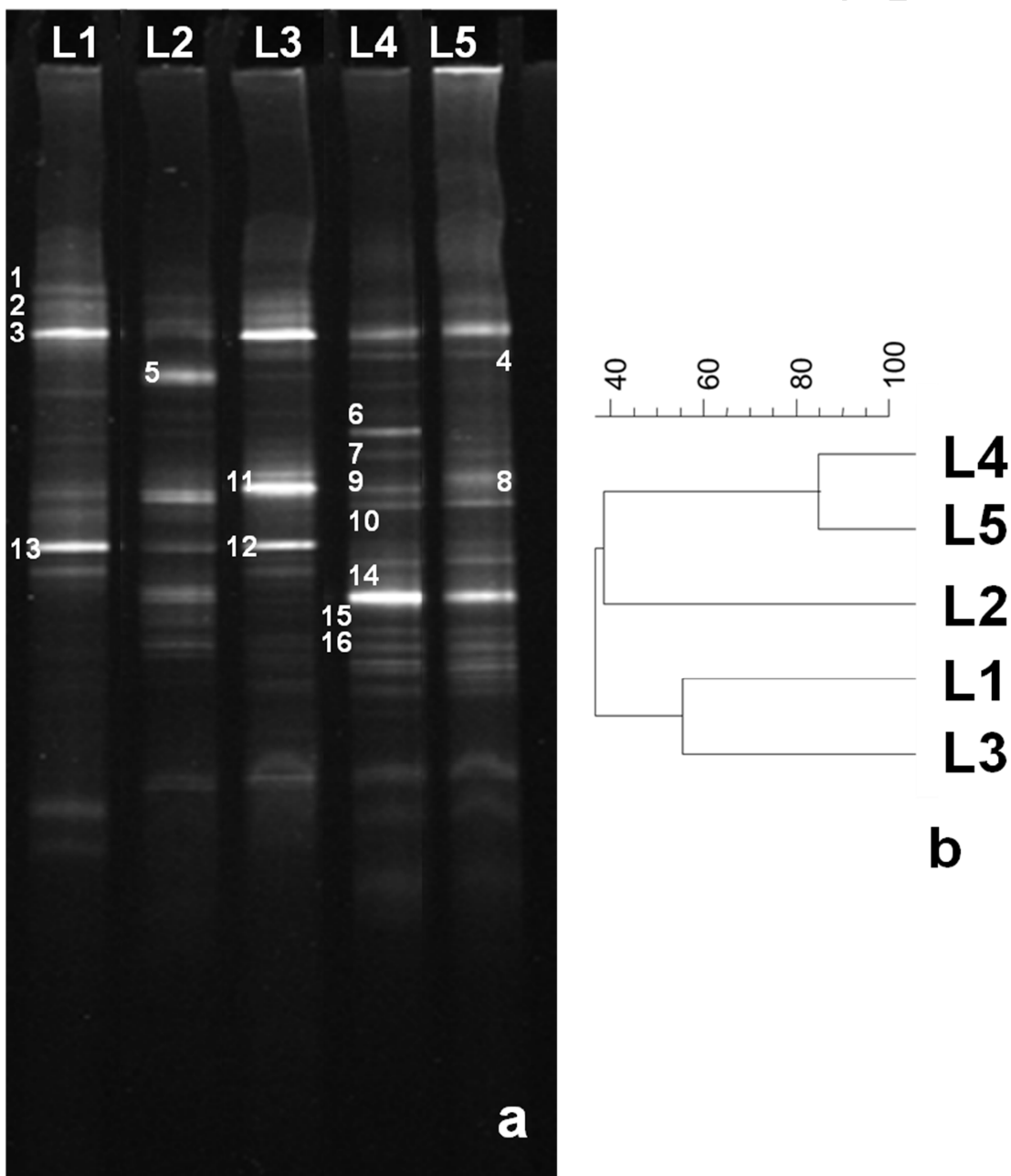
366

367

Figure 4. Color of elemental Se (a) produced, SEM images (b) and EDXS analyses (c) of effluents from thermophilic (1) and mesophilic (2) UASB reactors sampled on day 98 of reactor operation (Selenate = 50 μM, Nitrate = 5000 μM, lactate = 13.8 mM). Please note that the color of the effluent of both UASB reactors was different from day 1 of the reactor operation.

368 **3.6 Microbial community analysis of the UASB reactor granules**

369 The DGGE clearly showed the differences between the bands of the anaerobic granules at
370 different operating temperatures as well as at different points of reactor operation (Figure
371 5a). The diversity analysis carried out suggested that the microbial community in both
372 reactors was only 40% similar after the addition of selenate for 18 days (end of period II)
373 (Figure 5b). The similarity of the microbial community increased to 80% at the end of
374 period V in both reactors after addition of nitrate (Figure 5b).



375

376 **Figure 5.** DGGE (a) and diversity analysis (b) of bacteria in both UASB reactors at
 377 different points of time during reactor operation: inoculated anaerobic granules (L1),
 378 mesophilic anaerobic granules at the end of period II (L2) and V (L4) and thermophilic
 379 anaerobic granules at the end of period II (L3) and V (L5).

380

381 Sequencing of the selected bands showed the presence of *Geovibrio ferrireducens* in the
 382 inoculum, at the end of period II in the thermophilic UASB reactor and in both UASB
 383 reactors at the end of period V (Figure 5a and Table 3). *Sulfurospirillum barnesii* and
 384 *Pseudomonas stutzeri* were found present in, respectively, the mesophilic and
 385 thermophilic UASB reactor, while *Desulfotomaculum nigrificans* was found present in the
 386 inoculum and in both reactors at the end of period II (Table 3).

387

388 **Table 3.** Presence of different microorganisms in the UASB reactors: inoculated anaerobic
 389 granules (L1), mesophilic anaerobic granules at the end of period II (L2) and V (L4) and
 390 thermophilic anaerobic granules at the end of period II (L3) and V (L5).

Band no. in DGGE (Figure 5a)	Microorganisms	L1	L2	L3	L4	L5
1	<i>Marinifilum flexuosum</i>	+	—	—	—	—
2	<i>Alkalitalea saponilacus</i>	+	—	+	+	—
3	<i>Geovibrio ferrireducens</i>	+	—	+	+	+
4	<i>Clostridium thermobutyricum</i>	—	—	—	—	+
5	<i>Sulfurospirillum barnesii</i>	—	+	—	—	—
6	<i>Cesiribacter andamanensis</i>	—	—	—	+	—
7	<i>Desulfurispirillum indicum</i>	—	—	—	+	—
8, 9, 11	<i>Pseudomonas stutzeri</i>	—	—	+	+	+
10	<i>Paracoccus denitrificans</i>	+	—	—	+	+
12	<i>Desulfotomaculum nigrificans</i>	+	+	+	—	—
13	<i>Odoribacter laneus</i>	+	—	+	—	—
14	<i>Denitrovibrio acetiphilus</i>	—	+	—	+	+
15	<i>Geovibrio thiophilus</i>	—	+	—	+	+
16	<i>Paracoccus versutus</i>	—	+	+	+	+

391

392 Upon the addition of nitrate during period III-V in both reactors, *Paracoccus denitrificans*,
393 present in the inoculum, but not detected in both UASB reactors at the end of period II,
394 was found again present in both UASB reactors at the end of period V (Table 3).
395 *Denitrovibrio acetiphilus*, initially present only in the mesophilic UASB reactor at the end of
396 period II, was found in both UASB reactors at the end of period V. *Pseudomonas stutzeri*,
397 which was found present only in the thermophilic UASB reactor at the end of period II, was
398 found present in both reactors at the end of period V. *Desulfurispirillum indicum*, a
399 selenate reducing bacterium, was detected in the mesophilic UASB reactor only at the end
400 of period V.

401

402 **4. Discussion**

403 **4.1 Biological removal of Se in UASB reactors**

404 This study demonstrated that a better total Se removal efficiency can be achieved in an
405 UASB reactor operating at thermophilic (55°C) as compared to mesophilic (30°C)
406 conditions when the influent selenate concentration is 50 µM (Figure 2a). The higher total
407 Se removal efficiency in the thermophilic UASB reactor was due to the lower BioSeNPs
408 (elemental Se) concentrations compared to mesophilic UASB reactor in the effluent (Table
409 2, Figure 2d). The absence of Se in the gas traps of both UASB reactors suggests that the
410 major selenate removal mechanism in both UASB reactors was selenate reduction to
411 elemental selenium and its subsequent retention in the bioreactor, as confirmed by the
412 different BioSeNPs concentration in the effluent of the UASB reactors (Figure 2d).

413

414 The lower concentration of BioSeNPs in the thermophilic UASB reactor effluent (Figure 2d,
415 Table 2) when compared to the effluent of the mesophilic UASB reactor was probably due
416 to the extracellular reduction of selenate to BioSeNPs under mesophilic conditions, as

417 indicated by the members of the microbial community (Figure 5, Table 3). *Sulfurospirillum*
418 *barnesii*, present in the mesophilic UASB reactor at the end of period II, produces
419 BioSeNPs extracellularly (Figure 5a, Table 3) (Oremland et al., 2004). *Pseudomonas*
420 *stutzeri*, present in the thermophilic reactor at the end of period II, reduces selenate
421 (Kuroda et al., 2011; Lortie et al., 1992); however, localization of the BioSeNPs formed in
422 this species have not yet been studied in detail (Figure 5a, Table 3).

423

424 The other possible reason for the lower BioSeNPs concentration in the effluent of the
425 thermophilic UASB reactor compared to the mesophilic UASB reactor can be the different
426 settling properties of the BioSeNPs produced under thermophilic conditions (nanorods)
427 and mesophilic conditions (nanospheres) (Figure 4b). BioSeNPs are known to interact with
428 cations, which were present in both UASB reactors, leading to a less negative ζ -potential
429 value resulting in a decrease in their colloidal stability and thus allowing them to settle
430 (Buchs et al., 2013; Jain et al., 2015a). The lowering of the ζ -potential depends on the
431 surface interactions of the cations with the BioSeNPs, which depend on the properties of
432 the BioSeNPs, including shape, size and surface charge. However, further research is
433 required to study the settling properties of differently shaped BioSeNPs in different
434 environmental and engineered settings.

435

436 It is interesting to note that at an influent concentration of 10 μM selenate, longer
437 adaptation times (9 days) were required for the thermophilic UASB reactor to achieve total
438 dissolved Se removal efficiencies comparable to those obtained instantaneous under
439 mesophilic conditions (Figures 2a, 2b). Surprisingly, this was not observed when the
440 reactors were restarted using a feed selenate concentration of 50 μM with fresh anaerobic
441 granules (Figures 3a, 3b). This can be attributed to the fact that the adaptation of

442 anaerobic granules to selenate fed to a continuous reactor has a positive dependence on
443 the Se loading rate at non-toxic influent selenate concentrations (Takada et al., 2008),
444 thus, making the adaptation by anaerobic granules faster.

445

446 **4.2 Effect of nitrate on Se removal**

447 Lai et al. (2014) demonstrated that the reduction of selenate is inhibited by the presence of
448 nitrate at surface loading rates larger than $81.4 \text{ m moles m}^{-2} \text{ d}^{-1}$ ($\text{NO}_3^- / \text{SeO}_4^{2-}$ ratio =
449 56.2; 714 μM nitrate fed to the reactor). In this study, the selenate reduction efficiency was
450 not affected by the presence of nitrate at a $\text{NO}_3^- / \text{SeO}_4^{2-}$ ratio of 100 in the mesophilic as
451 well as thermophilic UASB reactor (Table S1, Figure S2a in SI). The higher selenate
452 removal efficiency ($> 99\%$) under thermophilic conditions can be due to presence of
453 *Pseudomonas stutzeri* (Figure 5a and Table 3), known for the reduction of selenate
454 (Kuroda et al., 2011; Lortie et al., 1992). The higher selenate removal efficiency under
455 mesophilic conditions ($> 98\%$) can be due to the presence of selenate-respiring
456 microorganisms e.g. *Sulfurospirillum barnesii* and *Desulfurspirillum indicum* (Figure 5a
457 and Table 3). Similar results were obtained in a *Sulfurospirillum barnesii* bioaugmented
458 anaerobic UASB sludge when the nitrate and sulfate concentrations were 1500 and 200
459 times in molar excess compared to selenate (Lenz et al., 2009). It is important to note that
460 unlike Lai et al. (2014), this study was carried out in presence of excess electron donor.

461

462 This study demonstrated that the presence of nitrate in the influent leads to excess release
463 of BioSeNPs in the effluent of both the reactors (Figures 2d, 3d and Table 2). In the
464 presence of nitrate as well, the thermophilic UASB reactor achieved $\sim 15\%$ higher total Se
465 removal efficiencies as compared to the mesophilic UASB reactor at a $\text{NO}_3^- / \text{SeO}_4^{2-}$ ratio
466 of 5000 in period V (Figure 3a and Table S1 in SI). The excess presence of BioSeNPs in

467 the effluent of the mesophilic UASB reactor can be partially attributed to the extracellular
468 production of BioSeNPs by selenate-respiring microorganisms such as *Desulfurispirillum*
469 *indicum* (Rauschenbach et al., 2011), found present in the mesophilic UASB reactor at the
470 end of period V (Tables 1 and 3).

471

472 The selenate-reducing microbial community is shaped by the presence of nitrate in a
473 hydrogen-based membrane biofilm reactor (Lai et al., 2014). In this study as well, the
474 addition of nitrate led to 80% similarity in the microbial community of both UASB reactors
475 at the end of period V, despite they were only 40% similar prior to NO_3^- feeding at the end
476 of period II (Figure 5b). The addition of nitrate also induced the growth of denitrifying
477 bacteria such as *Denitrovibrio acetiphilus* and *Paracoccus denitrificans* (Table 3).

478

479 **4.3 Se speciation**

480 The presence of volatile Se fractions in the gas traps was negligible (< 5 μg of Se was
481 trapped in the gas traps for the entire period) at 30°C, as observed in earlier studies with
482 UASB (Lenz et al., 2008a, 2008b) and activated sludge (Jain et al., 2016) reactors.
483 Interestingly, it was also negligible at 55°C (< 5 μg of Se was trapped in the gas traps for
484 the entire period), suggesting that the formation of alkylated compounds is not related to
485 the temperature within the range investigated.

486

487 The selenide formation was also not observed during the long term reactor operation, as
488 the concentration of Se in the second gas trap was negligible for both UASB reactors. This
489 is plausible as microorganisms such as *Sulfurospirillum barnesii*, *Bacillus*
490 *arsenicosenatis*, and *Selenihalanaerobacter shriftii* are not known to readily produce
491 selenide (Herbel et al., 2003). Nevertheless, it is also possible that some selenide was

492 formed in the reactor mixed liquor and then quickly oxidized to elemental Se or precipitate
493 as metal selenide, and thus remained undetectable in both the liquid and gas phase.

494

495 **4.4 Practical implications**

496 This study showed the thermophilic UASB reactors can treat hot selenate and nitrate
497 contaminated wastewater, e.g. flue gas desulfurization scrubbing waters that have an
498 adiabatic temperature of about 55°C (Akiho et al., 2010; Higgins et al., 2008), without the
499 need to cool down the scrubbing water. Besides, a 10-15% higher total Se efficiency was
500 achieved in the thermophilic UASB reactor when compared to the mesophilic UASB
501 reactor. This difference may seem marginal in terms of percentage, however, a 10%
502 difference corresponds to 395 $\mu\text{g L}^{-1}$ or 1185 $\mu\text{g L}^{-1} \text{d}^{-1}$. Similarly, a 15% difference, as
503 observed in period V, would translate to 593 $\mu\text{g L}^{-1}$ or 1778 $\mu\text{g L}^{-1} \text{d}^{-1}$. This became even
504 more significant when considering that the flue gas desulfurization wastewater discharge
505 criterion is 5 $\mu\text{g L}^{-1}$ (0.063 μM) (US EPA, 2015).

506

507 A simple cost-benefit analysis was carried out considering the base cost of 0.25€ per kg of
508 Se of a biological selenium removal technology comprising of a series of anaerobic bed
509 reactors operating at 15°C coupled with sand filtration prior to discharge (MSE Technology
510 Applications Inc., 2001). Assuming the cost of electricity to be 0.075 € per kWh and the
511 thermal efficiency 95%, the cost for treating 1Kg of Se in the mesophilic and thermophilic
512 UASB reactor, respectively, is 0.51 and 1.06€. Though the removal cost of Se treatment is
513 higher for thermophilic conditions, the higher Se removal efficiency of the thermophilic
514 UASB reactor would ensure lower post treatment cost to meet the 5 $\mu\text{g L}^{-1}$ (0.063 μM)
515 discharge criterion. Thus, a holistic view of the complete system composed of the
516 bioreactor and secondary treatment step is required to fully identify the operating costs of

517 such systems. Future work needs to focus on understanding the limitations of a UASB
518 reactor to internal hydrodynamics with emphasis on recovering the BioSeNPs. Low-cost
519 electron donors, such as methane or ethanol, need to be tested to determine the
520 maximum selenate and total Se removal rates while attempting to reduce the costs of the
521 electron donor.

522

523 **5. Conclusions**

- 524 • Thermophilic UASB reactors achieved 10-15% higher total Se removal efficiency
525 compared to the mesophilic UASB reactor
- 526 • Thermophilic conditions (55°C) led to the formation of different shaped BioSeNPs in
527 the thermophilic (nanorods) and mesophilic (nanospheres) UASB reactors
- 528 • Extracellular BioSeNPs producing selenate-respiring microorganisms (e.g.
529 *Sulfurospirillum barnesii*) in the mesophilic UASB reactor is one of the reasons for
530 its lower efficiency
- 531 • Addition of nitrate triggers the higher concentration of BioSeNPs in the effluent of
532 both the UASB reactors

533

534 **Supporting information**

535 The SI contains extra figures with experimental data as noted in the text.

536

537 **Acknowledgements**

538 The authors thank Ferdi Battles (UNESCO-IHE, The Netherlands) for help in reactor
539 construction, Berend Lolkema (UNESCO-IHE, The Netherlands) and Frank Wiegman
540 (UNESCO-IHE, The Netherlands) for GF-AAS. The authors would also like to thank

541 Norbert Jordan (HZDR, Dresden), Stephan Weiss (HZDR, Dresden) and René Hübner
542 (HZDR, Dresden) for carrying out SEM-EDXS of the samples.

543

544 **Author Contributions**

545 The manuscript was written through contributions of all authors. All authors have given
546 approval to the final version of the manuscript.

547

548 **Funding Sources**

549 This research was supported through the Erasmus Mundus Joint Doctorate Environmental
550 Technologies for Contaminated Solids, Soils, and Sediments (ETeCoS³) (FPA n°2010-
551 0009) and the Lifelong Learning Program (LLP) Erasmus Placement (2013), both financed
552 by the European Commission.

553

554 **References**

- 555 Akiho, H., Ito, S., Matsuda, H., 2010. Effect of oxidizing agents on selenate formation in a
556 wet FGD. *Fuel* 89, 2490–2495.
- 557 Buchs, B., Evangelou, M.W.-H., Winkel, L., Lenz, M., 2013. Colloidal properties of
558 nanoparticulate biogenic selenium govern environmental fate and bioremediation
559 effectiveness. *Environ. Sci. Technol.* 47, 2401–2407.
- 560 Chung, J., Nerenberg, R., Rittmann, B.E., 2006. Bioreduction of selenate using a
561 hydrogen-based membrane biofilm reactor. *Environ. Sci. Technol.* 40, 1664–71.
- 562 Herbel, M.J., Blum, J.S., Oremland, R.S., Borglin, S.E., 2003. Reduction of elemental
563 selenium to selenide: experiments with anoxic sediments and bacteria that respire Se-
564 oxyanions. *Geomicrobiol. J.* 20, 587–602.
- 565 Higgins, T., Givens, S., Sandy, T., 2008. FGD wastewater treatment still has a ways to go.
566 *Power Eng.* [http://www.power-eng.com/articles/print/volume-112/issue-1/features/fgd-
567 wastewater-treatment-still-has-a-ways-to-go.html](http://www.power-eng.com/articles/print/volume-112/issue-1/features/fgd-wastewater-treatment-still-has-a-ways-to-go.html), Accessed on: 18/01/2016
- 568 Jain, R., Jordan, N., Schild, D., van Hullebusch, E.D., Weiss, S., Franzen, C., Farges, F.,
569 Hübner, R., Lens, P.N.L., 2015a. Adsorption of zinc by biogenic elemental selenium
570 nanoparticles. *Chem. Eng. J.* 260, 855–863.
- 571 Jain, R., Jordan, N., Weiss, S., Foerstendorf, H., Heim, K., Kacker, R., Hübner, R.,
572 Kramer, H., van Hullebusch, E.D., Farges, F., Lens, P.N.L., 2015b. Extracellular
573 polymeric substances govern the surface charge of biogenic elemental selenium
574 nanoparticles. *Environ. Sci. Technol.* 49, 1713–1720.
- 575 Jain, R., Matassa, S., Singh, S., Hullebusch, E.D. Van, Esposito, G., Farges, F., Lens,
576 P.N.L., 2016. Reduction of selenite to elemental selenium nanoparticles by activated
577 sludge under aerobic conditions. *Environ. Sci. Pollut. Res.* 23, 1193–1202.

- 578 Jain, R., Seder-Colomina, M., Jordan, N., Dessi, P., Cosmidis, J., van Hullebusch, E.D.,
579 Weiss, S., Farges, F., Lens, P.N.L., 2015c. Entrapped elemental selenium
580 nanoparticles affect physicochemical properties of selenium fed activated sludge. J.
581 Hazard. Mater. 295, 193–200.
- 582 Kuroda, M., Notaguchi, E., Sato, A., Yoshioka, M., Hasegawa, A., Kagami, T., Narita, T.,
583 Yamashita, M., Sei, K., Soda, S., Ike, M., 2011. Characterization of *Pseudomonas*
584 *stutzeri* NT-I capable of removing soluble selenium from the aqueous phase under
585 aerobic conditions. J. Biosci. Bioeng. 112, 259–64.
- 586 Lai, C.Y., Yang, X., Tang, Y., Rittmann, B.E., Zhao, H.P., 2014. Nitrate shaped the
587 selenate-reducing microbial community in a hydrogen-based biofilm reactor. Environ.
588 Sci. Technol. 48, 3395–3402.
- 589 Lee, J.-H., Han, J., Choi, H., Hur, H.-G., 2007. Effects of temperature and dissolved
590 oxygen on Se(IV) removal and Se(0) precipitation by *Shewanella* sp. HN-41.
591 Chemosphere 68, 1898–905.
- 592 Lenz, M., Enright, A.M., O'Flaherty, V., van Aelst, A.C., Lens, P.N.L., 2009.
593 Bioaugmentation of UASB reactors with immobilized *Sulfurospirillum barnesii* for
594 simultaneous selenate and nitrate removal. Appl. Microbiol. Biotechnol. 83, 377–88.
- 595 Lenz, M., Hullebusch, E.D. Van, Hommes, G., Corvini, P.F.X., Lens, P.N.L., 2008a.
596 Selenate removal in methanogenic and sulfate-reducing upflow anaerobic sludge bed
597 reactors. Water Res. 42, 2184–2194.
- 598 Lenz, M., Lens, P.N.L., 2009. The essential toxin: the changing perception of selenium in
599 environmental sciences. Sci. Total Environ. 407, 3620–33.
- 600 Lenz, M., Smit, M., Binder, P., van Aelst, A.C., Lens, P.N.L., 2008b. Biological alkylation
601 and colloid formation of selenium in methanogenic UASB reactors. J. Environ. Qual.
602 37, 1691–700.
- 603 Lortie, L., Gould, W.D., Rajan, S., McCready, R.G., Cheng, K.J., 1992. Reduction of
604 selenate and selenite to elemental selenium by a *Pseudomonas stutzeri* isolate. Appl.
605 Environ. Microbiol. 58, 4042–4.
- 606 MSE Technology Applications Inc., 2001. Selenium treatment/removal alternatives
607 demonstration project: mine waste technology program activity III , Project 20,
608 National Service Center for Environmental Publications, US EPA,
609 doi:10.1007/s10811-012-9939-5.
- 610 Nancharaiah, Y. V, Lens, P.N.L., 2015. Ecology and biotechnology of selenium-respiring
611 bacteria. MMBR 79, 61–80.
- 612 Oremland, R.S., Herbel, M.J., Blum, J.S., Langley, S., Beveridge, T.J., Ajayan, P.M.,
613 Sutto, T., Ellis, A. V, Curran, S., 2004. Structural and spectral features of selenium
614 nanospheres produced by Se-respiring bacteria. Appl. Environ. Microbiol. 70, 52–60.
- 615 Rauschenbach, I., Narasingarao, P., Haggblom, M.M., 2011. *Desulfurispirillum indicum* sp.
616 nov., a selenate- and selenite-respiring bacterium isolated from an estuarine canal. Int
617 J Syst Evol Microbiol 61, 654–658.
- 618 Roest, K., Heilig, H.G.H.J., Smidt, H., de Vos, W.M., Stams, A.J.M., Akkermans, A.D.L.,
619 2005. Community analysis of a full-scale anaerobic bioreactor treating paper mill
620 wastewater. Syst. Appl. Microbiol. 28, 175–85.
- 621 Staicu, L.C., van Hullebusch, E.D., Oturan, M. a., Ackerson, C.J., Lens, P.N.L., 2015.
622 Removal of colloidal biogenic selenium from wastewater. Chemosphere 125, 1–9.
- 623 Stams, A.J.M., Grolle, K.C.F., Frijters, C.T.M.J., Van Lier, J.B., 1992. Enrichment of
624 thermophilic propionate-oxidizing bacteria in syntrophy with *Methanobacterium*
625 *thermoautotrophicum* or *Methanobacterium thermoformicum*. Appl. Environ.
626 Microbiol. 58, 346–352.
- 627 Takada, T., Hirata, M., Kokubu, S., Toorisaka, E., Ozaki, M., Hano, T., 2008. Kinetic study

- 628 on biological reduction of selenium compounds. *Process Biochem.* 43, 1304–1307.
- 629 Tam, K., Ho, C.T., Lee, J.-H., Lai, M., Chang, C.H., Rheem, Y., Chen, W., Hur, H.-G.,
630 Myung, N. V., 2010. Growth mechanism of amorphous selenium nanoparticles
631 synthesized by *Shewanella* sp. HN-41. *Biosci. Biotechnol. Biochem.* 74, 696–700.
- 632 Tanji, K.K., Kielen, N.C., 2003. Agricultural drainage water management in arid and semi-
633 arid areas. FAO corporate document repository, FAO irrigation and drainage paper
634 61, Chapter 8, pp:101-106, ISBN 92-5-104839-8,
635 <http://www.fao.org/docrep/005/y4263e/y4263e00.HTM>, Accessed on: 18/01/2016.
- 636 US EPA, Drinking water contaminants, [http://www.epa.gov/your-drinking-water/table-](http://www.epa.gov/your-drinking-water/table-regulated-drinking-water-contaminants#Inorganic)
637 [regulated-drinking-water-contaminants#Inorganic](http://www.epa.gov/your-drinking-water/table-regulated-drinking-water-contaminants#Inorganic), Accessed on: 18/01/2016.
- 638 US EPA, 2015. Effluent limitations guidelines and standards for the steam electric power
639 generating point source category. *Federal Register.* 80, 212, 67900,
640 <https://www.gpo.gov/fdsys/pkg/FR-2015-11-03/pdf/2015-25663.pdf>, Accessed on:
641 18/01/2016.

Highlights

UASB reactor at 55°C achieves a 10-15% higher total Se removal efficiency than at 30°C

BioSeNPs produced at 55°C are nanorods, whereas nanospheres at 30°C

Adding NO_3^- to the feed decreases the Se removal efficiency